

Self-Generation of Microwave Magnetic Envelope Soliton Trains in Yttrium Iron Garnet Thin Films

Boris A. Kalinikos,* Nikolai G. Kovshikov,* and Carl E. Patton

Department of Physics, Colorado State University, Fort Collins, Colorado 80523

(Received 26 September 1997)

The self-generation of microwave magnetic envelope solitons in magnetic films has been realized for the first time. Solitons with a width of 20 ns and a carrier frequency of 5.1555 GHz were generated for the magnetostatic backward volume wave (MSBVW) configuration in a 5.2 μm thick yttrium iron garnet film. The film and MSBVW propagation structure were part of a ring with an overall gain of +4 dB. Pulse modulation at 10 MHz provided the interrupted feedback and the active mode locking which was needed to produce a stable and continuous stream of self-generated soliton pulses. Pulse width and phase measurements confirmed the soliton nature of the self-generated pulses. [S0031-9007(98)06049-9]

PACS numbers: 75.30.Ds, 76.50.+g, 85.70.Ge

It is well known that solitons are eigenmode solutions to many nonlinear equations (see, e.g., [1–3]). Under the proper conditions, it should be possible for such eigenmodes to self-generate. Most soliton experiments to date, however, have involved the application of input pulse signals and the observation of the soliton pulses which evolve as a result of these inputs. Many such experiments have been done for microwave magnetic envelope (MME) solitons in magnetic films of yttrium iron garnet (YIG) (see, e.g., [4–11] and literature therein). In all of these experiments, externally applied microwave pulses were used to produce the solitons.

This Letter reports the first experimental demonstration of the self-generation of MME solitons. Through the use of gated feedback synchronized to the propagation time of the MME pulses in the YIG film, solitons were self-generated and synchronized to the 10 MHz gate signal. The self-generated soliton pulse sequence obtained in this way could be extended indefinitely. The measured pulse amplitude-width characteristics and phase profiles demonstrate the soliton character of these self-generated pulse signals, produced without any input pulse whatsoever.

The experiments were made for magnetostatic backward volume wave (MSBVW) excitations with positive dispersion and negative nonlinear frequency response. These signals were set up in a long and narrow, 50 by 1.5 mm, 5.2 μm thick (111) YIG film strip with input and output transducers spaced 1.75 mm apart. The YIG film had a narrow ferromagnetic resonance linewidth and unpinned surface spins. A static magnetic field of 1127 Oe was applied parallel to the long direction of the film. The MSBVW structure was connected in a closed ring with a microwave switch and amplifier. The generation of a stable sequence of soliton pulses was then accomplished by a regular interruption of the feedback circuit every 100 ns, the same as the delay time for the MSBVW signal around the ring. The above arrangement produced self-generated solitons at the chosen repetition rate. The soli-

ton carrier signal was measured to be 5.1555 GHz, and the soliton envelope width at half amplitude was 20 ns.

Figure 1 shows the soliton pulse train generator setup with the YIG film structure, a variable attenuator, a microwave switch S , and a microwave amplifier in a feedback ring as shown in the dashed line box. Provision is made for a low power cw microwave input signal to the loop through directional coupler DC-1. The cw input signal, when applied, and the signals before and after the YIG film structure are monitored through directional couplers DC-2, DC-3, and DC-4, respectively.

If pulse generation starts in the ring, one would obtain a repetitive sequence of the pulses with a separation in time equal to the combined delay time of the MSBVW pulse signal in the YIG strip and the electronic delay time of the ring. If the total ring gain factor G is sufficiently large, one may further obtain a sequence of soliton pulses without decay. The soliton response is self-limiting, so that a suitable gain can yield soliton self-generation. The gain needed to achieve such self-generation, however, will usually yield parasitic oscillations as well. These oscillations are suppressed by opening the switch S in

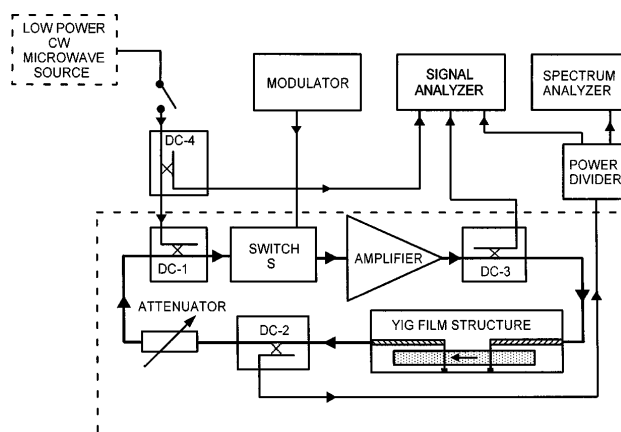


FIG. 1. Diagram of YIG film system for the self-generation of microwave magnetic envelope soliton signals.

synchronization with the overall delay time for the signal in the ring. This synchronized switch operation serves the additional function of active mode locking.

The critical issue for the above scenario concerns the physical basis for any such self-generation process. The well-known concept of modulational instability provides such a basis. Many nonlinear systems exhibit such an instability. The typical effect is a modulation of the steady state response as a result of the interplay between nonlinearity and dispersion (see, e.g., [3]). In a dissipative medium, the spontaneous modulation in combination with an external system modulation can result in the development of a periodic soliton pulse train if two criteria are satisfied: (1) Dispersion and nonlinearity have different signs such that the so-called Lighthill criterion is satisfied; (2) the power can attain a level at the threshold of the modulational instability.

The first criterion is readily met by the MSBVW excitations. For such signals, the dispersion coefficient $D = \partial\omega_k^2/\partial k^2$, where ω_k and k denote the carrier frequency and wave number, respectively, is positive. The nonlinear response coefficient N , which defines the shift in ω_k as the amplitude of the signal is increased, is negative. As demonstrated by the references cited above, when the Lighthill criterion, $DN < 0$, is satisfied, a compensation between the dispersion and the nonlinear frequency shift at high power can lead to formation of stable soliton pulses from suitable input pulses. The second criterion is easily met if the usual MSBVW decay due to relaxation is compensated by amplification in the ring.

As indicated above, the experimental parameters already cited yielded self-generated soliton pulses at a carrier frequency of 5155.5 MHz. The measured upper limit MSBVW passband frequency with the given operating parameters was 5230.9 MHz. For the above conditions, a YIG saturation induction $4\pi M_s = 1750$ G, and a gyromagnetic ratio γ defined by $|\gamma|/2\pi = 2.8$ GHz/kOe, an add-on static field increment of 30 Oe was needed to match the theoretical band edge to the measurement. A field of this order from magnetocrystalline anisotropy and strain is expected. With this adjustment, the theory gives a lowest order dispersion branch 5155.5 MHz operating point k value of 205 rad/cm and a theoretical group velocity, $v_g = |\partial\omega_k/\partial k|$, of 2.19×10^6 cm/s. This velocity is in good agreement with the measured soliton velocity and the 80 ns magnetostatic wave delay in the experiment.

Measurements were carried out in two stages. First, power vs frequency characteristics of the MSBVW ring structure were measured for a low cw input power and different gain settings. These measurements were done with switch S closed, so that the feedback was always in place. Second, self-generated soliton pulses and phase profiles, as well as the frequency spectra for these repetitive pulse signals, were measured. For these measurements, the switch was pulse modulated with a period of 100 ns. The second series of measurements was

done both with and without a low power cw reference microwave signal introduced into the ring. The cw signal was necessary only for the measurement of phase profiles.

The ring gain was varied through the attenuator in Fig. 1. Typical cw power vs frequency data are given in the graphs of Figs. 2(a)–2(c). The graph of Fig. 2(d) shows the power-frequency spectrum for a typical self-generated soliton signal. This graph will be discussed shortly. The power-frequency characteristics shown in Figs. 2(a)–2(c) were obtained for different values of the net ring gain G , as indicated. These gain factors were determined empirically, with $G = 0$ dB defined as the point in which the ring would just break into oscillation. This occurred for the 5.1555 GHz spike indicated by the solid circle in Fig. 2(c). The gain factors of -23.7 dB for Fig. 2(a) and -2.7 dB for Fig. 2(b) are relative to this critical gain for Fig. 2(c). The corresponding peak in Fig. 2(d) is indicated by a solid square.

For Fig. 2(a) and $G = -23.7$ dB, the feedback is essentially zero. The response here, therefore, shows a power-frequency profile which is typical for an MSBVW transmission line with no feedback. Over the gain range in Figs. 2(b) and 2(c), it is clear that the feedback results in sharp, well-defined spikes in the power-frequency response.

The different frequency values in Fig. 2 correspond, of course, to different MSBVW wave numbers. The spikes in Figs. 2(b) and 2(c) correspond to frequency points for

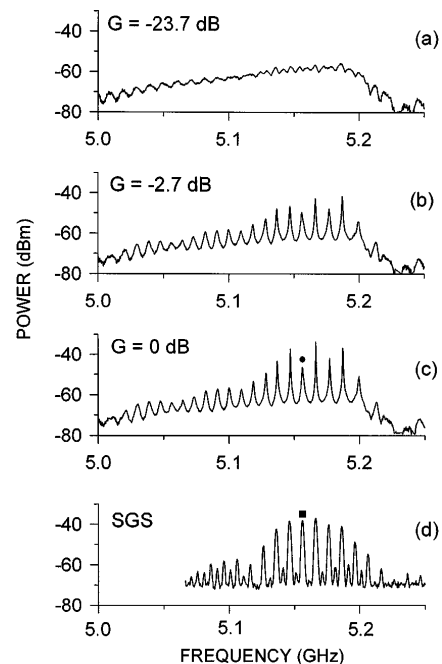


FIG. 2. Graphs (a)–(c) show cw power vs frequency response characteristics of the MSBVW ring structure for different ring gain factors as indicated and discussed in the text. Graph (d) shows the power-frequency spectrum for a typical self-generated soliton pulse sequence. The solid circle in (c) and solid square in (d) indicate the 5.1555 GHz spike and peak, respectively, as discussed in the text.

which the phase matching condition

$$k(\omega)L + \phi = 2\pi n \quad (1)$$

is satisfied, where L denotes the transducer spacing for the MSBVW structure, ϕ denotes the electronic phase associated with the rest of the ring, and n is an integer.

The frequency spike points which satisfy Eq. (1) represent phase locked resonances for the circulating self-generated cw signal in the ring. It is clear from Figs. 2(b) and 2(c) that there are many such points within the MSBVW passband. It is important to emphasize that the power-frequency spectrum in Fig. 2(d) is *self-generated*. This profile is *not* obtained with a frequency swept input signal. Here, there is *no* input signal. This self-generated cw signal in Fig. 2(d) is simultaneously operating at a number of resonance frequencies which satisfy Eq. (1).

The ring gain is also critical. For the type of clean resonance responses shown in the graphs of Figs. 2(b) and 2(c), the gain factor must not be too small or too large. If the gain G was increased above the level set for Fig. 2(c), the response would break into oscillation. The actual gain factor will be different, of course, for the different frequency spikes. For $G > 0$ dB, the oscillation was found to begin for a spike positioned at 5155.5 MHz. This spike is identified in Fig. 2(c) by the solid circle.

Turn now to the series of experiments for which the feedback connection around the ring was periodically interrupted at a pulse modulation rate of 100 ns. For each cycle, the feedback loop was closed for 22 ns. In other words, the modulation signal consisting of a sequence of 22 ns wide rectangular pulses with a repetition frequency of 10 MHz was applied to the switch. Changes in the switch closed time could be used to modify the shape as well as the power-frequency spectrum of the self-generated pulse signal in the ring. The 22 ns closed time appeared to be the optimal time for the self-generation of single soliton profiles. As already indicated, the modulation period of 100 ns matched the around-the-ring propagation time of the signal. This match was needed to produce the active mode locking which leads to the self-generation of the MME solitons. This modulation period is given by

$$t_m = L/v_g + t_e, \quad (2)$$

where L/v_g gives the MSBVW propagation time in the YIG film, and t_e is the electronic delay for the rest of the ring. For these experiments, L/v_g and t_e were 80 and 20 ns, respectively.

The self-generation of solitons was achieved by adjusting the modulation period to match t_m and reducing the attenuation to give enough gain to exceed the modulational instability threshold. The applied modulation frequency $f_m = 1/t_m = 10$ MHz gave the needed timing. This frequency corresponds to the frequency separation of the spikes shown in Figs. 2(b) and 2(c). Simultaneous with the measurements of the amplitude and phase profiles of the self-generated pulse sequences, power-frequency spec-

tra for these signals were measured at the output of the YIG film structure with a spectrum analyzer. A typical spectrum for the pulse signals is shown in the graph of Fig. 2(d). The frequency peaks for the pulse signal exactly match the frequency spikes from the cw measurements.

Some representative data with the 10 MHz modulation applied to the switch are shown in Fig. 3. The ring gain for these data was set at $G = +4$ dB. The graphs of Figs. 3(a) and 3(b) show detected voltage vs time signals from the microwave analyzer. Figure 3(a) was obtained with an isolated ring and no external microwave input signal whatsoever. Figure 3(c) shows phase profiles. The data in Figs. 3(b) and 3(c) were obtained with a low power, 0.2 mW cw microwave signal at 5.1555 GHz applied to the ring through coupler DC-1 in Fig. 1. This input was needed only for the synchronization required for the phase measurements. The close match between the traces in Figs. 3(a) and 3(b) shows that this additional signal did not affect the shape of the ring signal in any way.

The graphs of Figs. 3(a) and 3(b) show that the self-generated ring signal consists of pulses approximately 20 ns in width with a repetition rate of 100 ns, the same as the matched modulation period and delay time t_m . It is to be emphasized that these pulses are entirely self-generated. The phase trace in Fig. 3(c) shows a 100 ns periodic structure as well. The abrupt 360° jumps represent instrumentation effects and have no physical significance. The key result here is in the plateau region of a constant phase which exactly tracks the peak portions of the voltage traces in the upper graphs. These regions of constant phase provide an unambiguous signature for the soliton nature of the pulses [11].

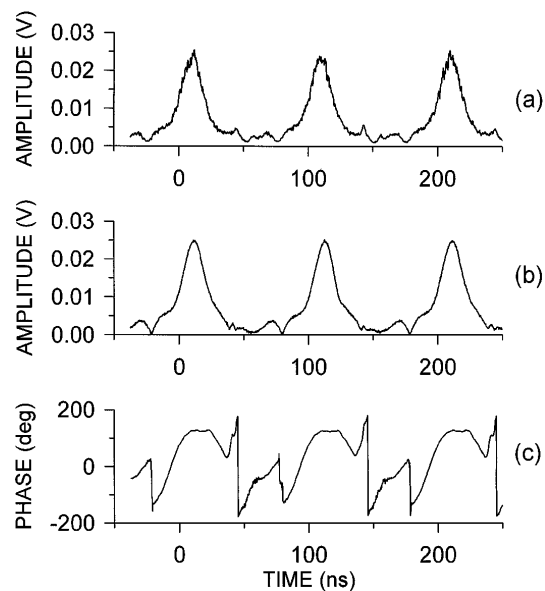


FIG. 3. Graphs (a) and (b) show detected microwave voltage vs time for the signal in the MSBVW ring structure for a 22 ns pulse modulation at 10 MHz and a ring gain of +4 dB. Graph (c) shows the phase profile corresponding to (b). For (b) and (c), a 0.2 mW cw microwave synchronization signal at 5.1555 GHz was applied to the ring as indicated in Fig. 1.

It is important to note that, in principle, any of the cw resonance frequencies could be used for a reference synchronization signal. The measurements showed, however, that the resonance at 5.1555 GHz was unique in providing a phase profile with a constant plateau over the center region of the voltage pulse profiles. One may conclude that this synchronization frequency is the carrier frequency of the self-generated soliton train.

The power-frequency spectrum of the ring signal shown in Fig. 3(b) was shown in the graph of Fig. 2(d). It is clear that the peaks in this spectrum match the spikes in the cw spectra in Figs. 2(b) and 2(c). These results demonstrate that the MSBVW ring arrangement with switch modulation which produces self-generated solitons has a power-frequency spectrum which coincides with the cw resonance frequencies of the ring. The 5.1555 GHz peak in Fig. 2(d) is indicated by the solid square.

Figure 4 shows a further example of the signals in the graphs of Figs. 3(b) and 3(c), but for an extended time scale. All operating conditions are the same as before. The main point of Fig. 4 is to demonstrate that the MSBVW ring with modulation can produce a *continuous, and essentially unlimited* sequence of soliton pulses.

The self-generated solitons result from the nonlinear interaction of the resonant MSBVW modes in the YIG film. The precisely timed modulation suppresses parasitic oscillation and promotes active mode locking. The mechanism is related to modulational instability, except that many resonance modes are involved. The number of the interacting modes is determined by the spectral bandwidth of the soliton and frequency separation of the resonance modes.

For this multimode process to work, the frequency spacing between neighboring resonance modes should be smaller than twice the modulational instability frequency f_0 of the system. Based on the nonlinear Schrödinger equation model (see, e.g., [3]), f_0 is equal to $u_0 v_g \sqrt{|N/D|}/\pi$, where u_0 is the signal amplitude. For $D = 520 \text{ cm}^2/\text{rad/s}$, $N = -9.9 \times 10^9 \text{ rad/s}$, and $u_0 = 0.014$, determined in the same way as in [10], f_0 is about 43 MHz. From theory, the maximum frequency

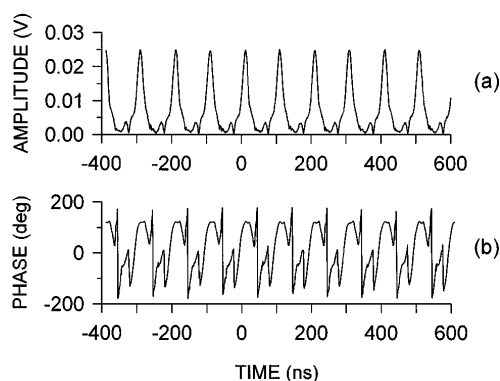


FIG. 4. Graphs (a) and (b) show detected microwave voltage and phase vs time from Figs. 3(b) and 3(c), but for a more extended time scale.

width for the modulational instability zone is equal to $2f_0$ or 86 MHz. The mode frequency spacing of 10 MHz, apparent from Fig. 2, and the corresponding modulation frequency of 10 MHz are well below this width.

The analysis also yields a prediction of the order one soliton width [e.g., see Eq. (1) in [10]]. For the experimental parameters, one obtains a theoretical soliton pulse width at half amplitude of 19.7 ns, which is in good agreement with the measured width of 20 ns. The shape of the pulses, the phase profiles of the pulses, and the width of the pulses all support the proposition that self-generated solitons are obtained.

In conclusion, this Letter reports the first results on the continuous self-generation of MME solitons in magnetic films. This self-generation takes place without any microwave pulse input whatsoever. The pulse signals represent the *bona fide* nonlinear eigenmodes of the system with the phase profiles and amplitude-width relationship expected for solitons. The self-generation process could be used to produce MME soliton trains of various pulse widths, carrier frequencies, and periodicities by the proper choice of film, field, and mode locking parameters.

This work was supported in part by the U.S. Army Research Office, Grant No. DAAH04-95-1-0325, the National Science Foundation, Grant No. DMR-9400276, the Russian Foundation for Basic Research, Grant No. 96-02-19515, and the NATO Linkage Grant Program, Grant No. HTECH.LG 970538.

*Permanent address: Saint Petersburg Electrotechnical University, 197376 Saint Petersburg, Russia.

- [1] M.J. Ablowitz and P.A. Clarkson, *Solitons, Nonlinear Evolutional Equations and Inverse Scattering* (Cambridge University Press, Cambridge, England, 1991).
- [2] G.L. Lamb, *Elements of Soliton Theory* (Wiley, New York, 1980).
- [3] M. Remoissenet, *Waves Called Solitons: Concepts and Experiments* (Springer-Verlag, Berlin, 1996).
- [4] B. A. Kalinikos, N.G. Kovshikov, and A.N. Slavin, *Zh. Eksp. Teor. Fiz.* **94**, 159 (1988) [*Sov. Phys. JETP* **67**, 303 (1988)].
- [5] M. Chen, M. A. Tsankov, J.M. Nash, and C.E. Patton, *Phys. Rev. Lett.* **70**, 1707 (1993).
- [6] M. Chen, M. A. Tsankov, J.M. Nash, and C.E. Patton, *Phys. Rev. B* **49**, 12773 (1994).
- [7] R. Marcelli and P. De Gasperis, *IEEE Trans. Magn.* **30**, 26 (1994).
- [8] J.M. Nash, C.E. Patton, and P. Kabos, *Phys. Rev. B* **51**, 15079 (1995).
- [9] N.G. Kovshikov, B.A. Kalinikos, C.E. Patton, E.S. Wright, and J.M. Nash, *Phys. Rev. B* **54**, 15210 (1996).
- [10] B.A. Kalinikos, N.G. Kovshikov, and C.E. Patton, *Phys. Rev. Lett.* **78**, 2827 (1997).
- [11] J.M. Nash, P. Kabos, R. Staudinger, and C.E. Patton, *J. Appl. Phys.* **83**, 2689 (1998).